DESIGN OF CREEP-RESISTANT FERRITIC-STEEL WELDING ALLOYS

H. K. D. H. BHADESHIA

University of Cambridge, Department of Materials Science and Metallurgy
Pembroke Street, Cambridge CB2 3QZ, U.K. www.msm.cam.ac.uk

ABSTRACT

Ferritic steels have relatively low thermal expansion-coefficients and can be alloyed to resist creep and oxidation during prolonged service at temperatures which can exceed 600°C. Their use in the construction of power plant places severe demands on welding alloys. The acceptability of a weld metal depends not only on the mechanical properties, but also on the ability of the welded joint to be heat-treated in a manner which is compatible with the parent materials.

There now exist methods available for estimating the microstructure, including the phases present, their fractions and chemical compositions as a function of time, temperature and alloying additions. Similarly, important mechanical properties such as strength, Charpy toughness and creep rupture strength can be modelled with an indication of uncertainty. The compatibility of weld metal with the steels being joined can also be addressed. It is hoped to review these and related phenomena in the context of power plant technologies.

INTRODUCTION

The efficient conversion of fossil fuels into electricity requires the development of steels which are capable of resisting creep and oxidation over long periods of time at temperatures in excess of 600°C. Since the alloys are joined by welding, there has to be a concomitant development of welding alloys and procedures.

The development and certification of alloys is in general a lengthy process. This paper focusses on methods for the prediction of the microstructure and properties of welding alloys for the power plant industries. We begin with a brief discussion of how a welding alloy might differ, metallurgically, from a creep-resistant steel.

COMPARISON OF WELD METAL TO WROUGHT STEEL

The microstructure of an as-deposited weld metal is naturally different from that of a wrought steel which has been through many stages of thermomechanical processing. These differences are vital in the case of structural steels used in the construction of buildings, oil platforms and the like, but not necessarily so for heat-resistant alloys. In the latter case, joints are subjected to quite severe post-weld heat treatments which essentially wipe out the original microstructure, leaving one which is tempered and similar to that of the steel plate. It is probably for this reason that the welding process itself is found not to influence the creep rupture life [1].

Weld metals and steels of matching composition are known to have similar creep rupture properties [2]. Indeed, the same structure-property models can be used to estimate weld metal performance [3,4]. The chemical compositions of weld metals and corresponding steel plates are not very different (Fig.1). Weld metals generally contain greater oxygen and nitrogen concentrations but the former should not affect creep resistance. Although differences in the nitrogen concentration are important, they can easily be taken into account both in predicting carbonitride formation and in the influence on mechanical properties [5].

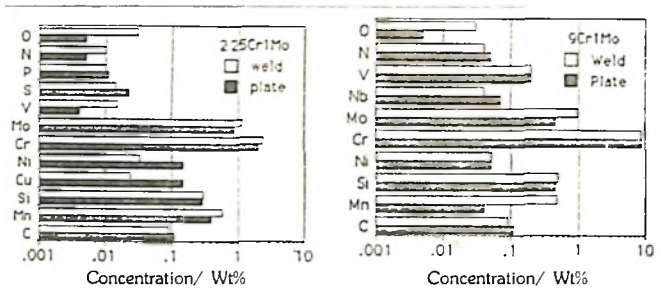

Fig. 1: Comparison of the chemical compositions of weld metal and corresponding wrought steel.

Some further evidence that the details of the initial microstructure frequently don't matter when considering the tempered state, comes from Baker and Nutting [6], who studied carbide precipitation reactions during the isothermal tempering of a $2\frac{1}{4}$Cr1Mo steel in the martensitic and bainitic conditions. Fig. 2 shows that whereas the kinetics of precipitation are not identical in the two cases, the differences are very small over the temperature range of interest (500–650°C).

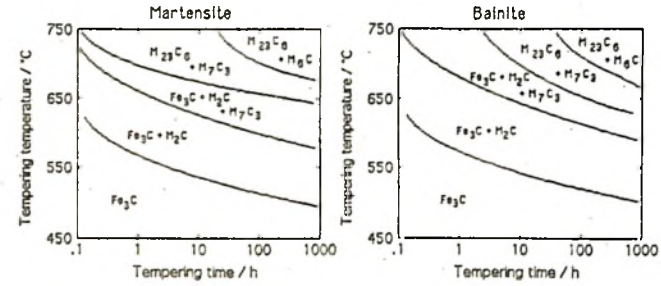

Fig. 2: Measured isothermal transformation diagrams for carbide precipitation reactions in $2\frac{1}{4}$ Cr1Mo steel. (a) Martensitic starting microstructure; (b) bainitic starting microstructure. Adapted from Baker and Nutting [6].

THE WELD-METAL MICROSTRUCTURE

There is a large range of heat-resistant steels and welding alloys [5]. The ones with the lowest solute concentrations might contain substantial quantities of allotriomorphic ferrite and some pearlite, but the vast majority have bainitic or martensitic microstructures in the normalised condition. After normalising the steels are severely tempered to produce a "stable" microstructure consisting of a variety of alloy carbides in a ferritic matrix. The task is therefore to model precipitation, coarsening and dissolution reactions.

Power plant alloys, whether they be for welding or otherwise, are not simple. They always contain more than one kind of precipitate, including a few metastable phases and some slow-forming intermetallic compounds. Because the precipitates form at somewhat different rates, it has been common practice to model the development of microstructure, one phase at a time. This is turn requires an empirical specification of the time at which one reaction gives way to another, and indeed of the point where a metastable phase begins to dissolve as a more stable precipitate forms. This clearly does not lead to a predictive model.

Recent advances in theory have meant that it is now possible to treat many transformations occurring simultaneously using a series of coupled kinetic-equations. This allows the reactions to occur in an interactive manner, thereby eliminating the need to start and stop any reaction – the transformations occur naturally as dictated by competition between the phases in their quest to approach equilibrium. A separate coarsening model is not needed when capillarity is included in the calculations. The method has been described elsewhere [7–14]; here we illustrate some of the important features of the results obtained.

The compositions of two power plant alloys used here for illustration purposes, are shown in Table 1. These alloys show similar precipitation *sequences* [6,7,8] but with vastly different rates. For example, at 600°C the time taken before $M_{23}C_6$ is observed is 10h in the 3Cr1.5Mo alloy [15] and in excess of 1000h in the $2\frac{1}{4}$ Cr1Mo steel [14]. These differences have never before been explained [7,8].

	C	N	Mn	Cr	Mo	Ni	V	Nb
2¼ Cr1Mo	0.15	–	0.50	2.12	0.9	0.17	–	–
3Cr1.5Mo	0.1	–	1.0	3.0	1.5	0.1	0.1	–

Table 1: Concentrations (in wt%) of the major alloying elements in the steels used to demonstrate the calculations.

MICROSTRUCTURE CALCULATIONS

A plot showing the calculated variation of volume fraction for each precipitate as a function of time at 600°C is shown in Fig. 3 for $2\frac{1}{4}$ Cr1Mo steel. All phases commence to form at time zero, albeit at different rates. Cementite is the fastest because it grows by a paraequilibrium mechanism in which the substitutional to iron atoms ratio remains constant

during transformation [16]. It follows that its initial composition will tend to change during service; although this is not obvious from Fig. 3, the progressive composition changes are accounted for in the calculations.

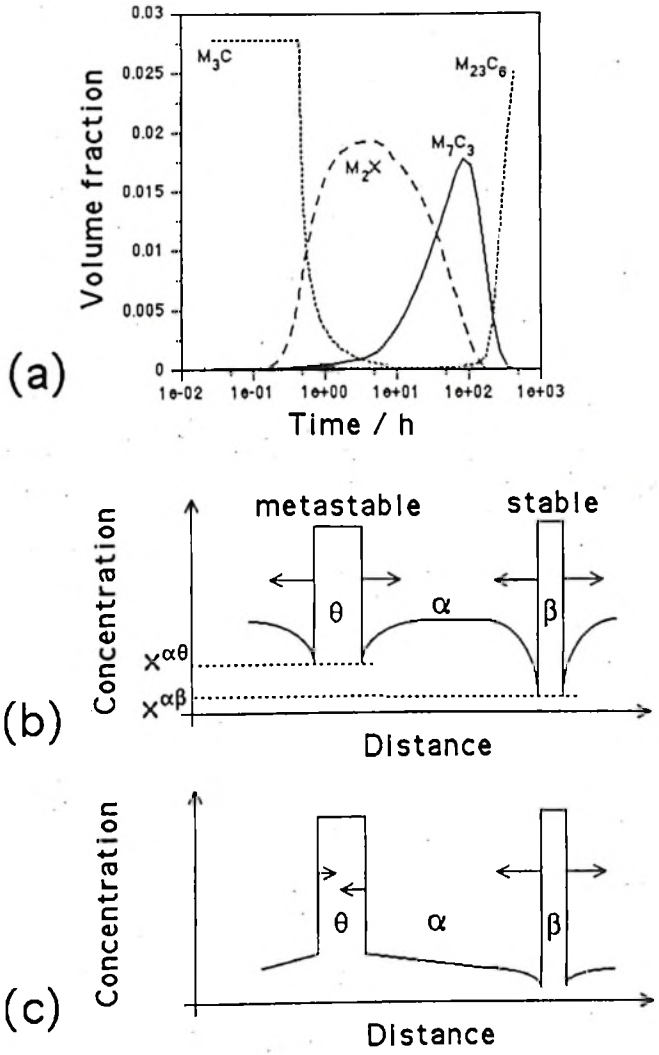

Fig. 3: (a) The predicted evolution of precipitate volume fractions at 600°C for $2\frac{1}{4}$ Cr1Mo steel [7,8]. (b) Interaction between metastable phase θ and the equilibrium phase β via their diffusion fields within the α matrix. The arrows indicate the directions in which the interfaces move. (b) illustrates the case prior to soft-impingement; (c) the case following soft-impingement.

The early stages of precipitation reactions in the solid-state are frequently dominated by metastable phases which are easy to nucleate but which do not lead to the maximum reduction in free energy. As the microstructure evolves, these phases are replaced eventually by thermodynamically more stable phases. Consider a situation in which the metastable phase θ and stable phase β precipitate from a supersaturated matrix α (Fig. 3b). It can be demonstrated that the concentration $x^{\alpha\theta}$ of solute in α which is in contact with θ will be higher than $x^{\alpha\beta}$. This does not matter at first because the diffusion fields of the individual precipitates do not overlap, *i.e.* soft-impingement has not yet occurred (Fig. 3b). However, as solute is depleted from the matrix α, the situation illustrated in Fig. 3c arises and although β continues to grow, θ dissolves.

Cementite is a metastable precipitate so it is not surprising that in Fig. 3a, it is replaced by M_2X. Similarly, M_2X dissolves as M_7C_3 precipitates, until at last the equilibrium precipitate $M_{23}C_6$ dominates the microstructure.

Consistent with experiments, the precipitation kinetics of $M_{23}C_6$ are predicted to be much slower in the $2\frac{1}{4}$Cr1Mo steel compared with 3Cr1.5Mo alloys (Fig. 4). One contributing factor is that in the $2\frac{1}{4}$Cr1Mo steel a relatively large volume fraction of M_2X and M_7C_3 form prior to $M_{23}C_6$. These deplete the matrix and therefore suppress $M_{23}C_6$ precipitation. The volume fraction of M_2X which forms in the 10CrMoV steel is relatively small, and there remains a considerable excess of solute in the matrix, allowing $M_{23}C_6$ to precipitate rapidly. Similarly, in the 3Cr1.5Mo steel the volume fractions of M_2X and M_7C_3 are insufficient to suppress $M_{23}C_6$ precipitation to the same extent as in the $2\frac{1}{4}$ Cr1Mo steel.

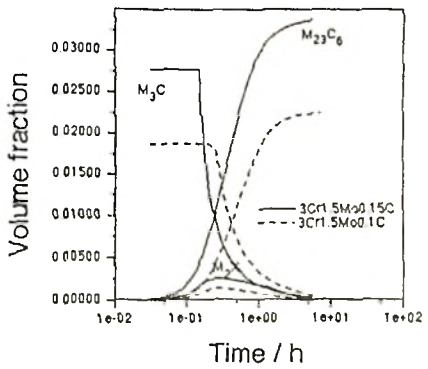

Fig. 4: The calculated evolution of precipitate volume fractions at 600°C for 3Cr1$\frac{1}{2}$Mo steel as a function of carbon concentrations and temperature [7,8,17].

$M_{23}C_6$ is frequently observed in the form of coarse particles which are less effective in hindering creep deformation. Delaying its precipitation would have the effect of stabilising the finer dispersions of M_2X and

MX to longer times with a possible enhancement of creep strength. Notice also how sensitive the results can be to the carbon concentration.

FACTORS AAECTING CREEP-RUPTURE STRENGTH

The basic principles of alloy design for creep resistance are well-established. The steels must have a stable microstructure which contains fine and closely-spaced precipitates to resist the motion of dislocations. Changes are nevertheless inevitable during service so there must be sufficient solid solution strengthening to ensure long term creep resistance. Fig. 5 shows the contributions made by a variety of factors to the creep rupture strength of $2\frac{1}{2}$Cr1Mo steels or weld metals, after 10^5 h service, as a function of temperature [18]. It is evident that the intrinsic strength of iron and contributions from solid-solution strengthening are dominant factors at long service times. The role of precipitates is diminished even further as the service temperature is increased, as is seen by comparing the pie-charts for 550°C and 600°C.

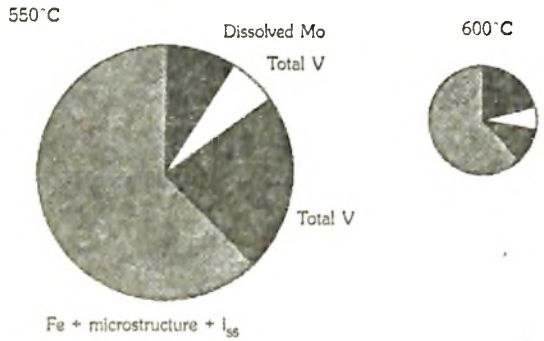

Fig. 5: Factorisation of the 10^5h creep-rupture strength of a $2\frac{1}{2}$Cr1Mo steel at the appropriate temperature. The term i_{ss} represents solid solution strengthening due to elements other than Mo or V. The diameter of each of the pie-charts scales with the creep rupture strength which is 79 and 30 MPa for 550°C and 600°C respectively [18].

We note that information about microstructure and properties is inherent in the chemical composition and heat treatment. Given this fact, most models for the creep rupture strength have the detailed chemical composition and processing as inputs. There may exist other independent variables that could be important in creep analysis, but these are for the moment neglected for two reasons. Firstly, the models are empirical and hence require experimental data; an over-ambitious list would reduce the available dataset since publications frequently do not report all of the necessary parameters. Secondly, the effect of any missing variables would be reflected in the uncertainties associated with the predictions. If the predictions are noisy then they can in future work be improved with carefully designed experiments.

NEURAL NETWORK MODELS

There is an excellent and well-proven method for creating quantitative models for complex mechanical properties. This is the neural network method which is able to capture almost arbitrarily non-linear relationships. Details of the method have been widely published [*e.g.* 19,20,21], but as an example, Fig. 6 illustrates the complexity of the surface that can be produced when representing the output (vertical axis) as a function of two inputs using a very simple neural network with just four "hidden nodes". With care, such non-linear functions can be used to fit complex and multi-dimensional data, whilst at the same time avoiding overfitting. The method is sufficiently sophisticated to give an indication of uncertainty in making predictions, such that the uncertainties can be large when calculating in regions of input space where experimental data are sparse or noisy.

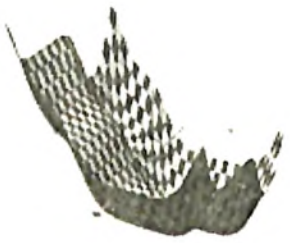

Fig. 6: Variation in the output (vertical axis) as a function of two input variables, the surface being represented with just four hyperbolic tangent functions.

CALCULATIONS OF WELD METAL CREEP-RUPTURE STRENGTH

The discussion in the earlier part of the paper, that steels and welding alloys of identical composition and heat treatment have similar creep rupture lives can be demonstrated by using a creep rupture model for wrought alloys to interpret published data on weld metals [22]. Such data are most reliable for the $2\frac{1}{4}$Cr1Mo type weld metals; the calculations are

therefore presented for the $2\frac{1}{4}$ Cr1Mo weld metal listed in Table 1, for a rupture life of 10^5 h.

Fig. 7 shows the encouraging agreement between the calculated [2,3] and measured [22] creep rupture lives of $2\frac{1}{4}$Cr1Mo welds. The predictions are made without any adjustment of the models, which did not interrogate any weld metal data during their creation. The results confirm that it is reasonable to assume that weld metal creep rupture life can be modelled on the basis of wrought steels. Of course, other properties such as creep ductility may be more sensitive to inclusion content in which case the weld metals should exhibit a lower ductility relative to the wrought steel.

The method can now be used to generate creep-rupture diagrams such as that illustrated in Fig. 8.

Fig. 9 shows that the same method can be used to estimate the creep-rupture life of modified 9CrMoW weld metal of composition listed in Table 2. The ability to predict the creep properties of these welds has direct industrial implications.

C	Si	Mn	P	S	Ni	Cr	Mo	W	V	Nb	N
0.07	0.20	1.01	0.006	0.004	0.36	8.94	0.48	1.62	0.09	0.04	0.032

Table 2: Chemical composition of gas tungsten arc weld metal, wt% [23]

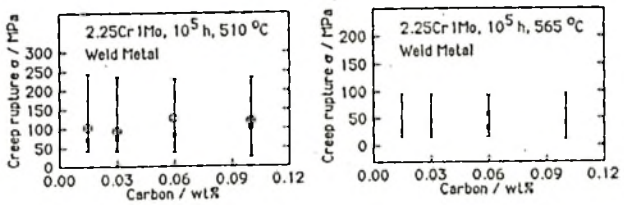

Fig. 7: Calculated (filled circles) with ± 1σ uncertainties and measured (open circles) stress rupture data for $2\frac{1}{4}$Cr1Mo weld metal.

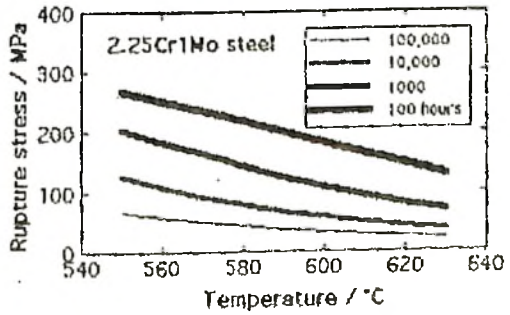

Fig. 8: Calculated stress rupture data for $2\frac{1}{4}$Cr1Mo weld metal.

MECHANICALLY-DISSIMILAR METAL JOINTS

Some of the alloys used in power plant operate under conditions where toughness is the prime requirement; one such alloy is the so-called $3\frac{1}{2}$ Ni steel (≈ 0.2C, 0.4Si, 0.4Mn, 1.75Cr, 0.4Mo, 0.2V, 3.9Ni wt%). It may be necessary to join this to a 10Cr1Mo creep-resistant alloy, with a requirement that post-weld heat treatment must not reduce the hardness of either steel should be in the range 256-290 HV [24]. Table 3 shows calculations of the heat-treatments which would result in the required hardness for each of the steels, assuming that martensite is generated in the heat-affected zones as a consequence of welding. A post-weld treatment at 700°C for 5 h would suit both alloys, but the time involved may be insufficient for large components to achieve thermal equilibrium. Based on these calculations, an alternative proprietary welding technology was developed.

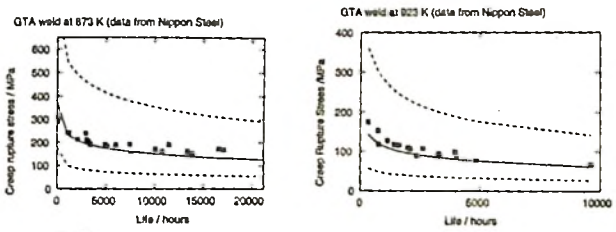

Fig. 9: (a) Calculated creep rupture strength at 873 K for the 9Cr weld deposit specified in Table 2. (b) Corresponding plot for 923 K. The experimental data are due to Naoi et al. [23]

Temperature	$3\frac{1}{2}$Ni	!0Cr1Mo	Temperature	$3\frac{1}{2}$Ni	!0Cr1Mo
600°C	450-600h	-	700°C	1-4 h	5-50 h
650°C	6-12 h	200-1000h	750°C	-	1-2 h

Table 3: Approximate times and temperatures required to produce a hardness between 265 and 290 HV [24]. A hyphen indicates that the required hardness is not achieved by the proposed heat-treatment.

CONCLUSIONS

The problems associated with the welding of creep-resistant steels are many, but there are now a variety of methods which can help ameliorate the difficulties. Two particular advances stand out in the set of tools available. First, modelling based on the thermodynamics and kinetics of solid-state transformations, can enable the evolution of microstructure to be estimated over the service life-time. Secondly, neural network models of complex mechanical properties are now making a

significant contribution in the quantitative design of creep-resistant welds and parent materials.

Furthermore, the combination of models can be used to assess the behaviour of dissimilar metal joints in which the component steels have different and sometimes incompatible responses to post-weld heat-treatment.

ACKNOWLEDGMENTS

I am grateful to the organisers of this conference for their invitation and to Drs Joe Robson, Dave Cole, Tracey Cool, Harsha Sree Lalam, Ananth Murugananth and Thomas Sourmail for many discussions on this subject.

REFERENCES

1. Lundin, C. D., Kelley, S. C., Menon, R. and Kruse, B. J. : *Welding Research Council bulletin 277,* New York (1986) 1-66
2. Bhadeshia, H. K. D. H. : *Trends in Welding Research,* eds. S.A. David, T. DebRoy, J.A. Johnson, H. B. Smartt and J. M. Vitek, ASM International, Ohio, (1999) 795-804.
3. Cole, D., Martin-Moran, C., Sheard, A., Bhadeshia, H. K. D. H. and MacKay, D. J. C.: *Science and Technology of Welding and Joining* **5** (2000) 81-89.
4. Cole, D. and Bhadeshia, H. K. D. H.: *Mathematical Modelling of Weld Phenomena-5, eds.* H. Cerjak and H. K. D. H. Bhadeshia, Institute of Materials, London (2001) 431-448.
5. Bhadeshia, H. K. D. H.: *ISIJ International* **41** (2001) 626-640.
6. Baker, R. G. and Nutting, J.: *Journal of the Iron and Steel Institute* **192** (1959) 257-268.
7. Robson, J. D. and Bhadeshia, H. K. D.H.: *Materials Science and Technology* **13** (1997) 631-644.
8. Robson, J. D. and Bhadeshia, H. K. D. H.: *Calphad* **20** (1996) 447-460
9. Bhadeshia, H. K. D. H: *Proceedings of Solid-Solid Phase Transformations'99 (JIMIC-3),* eds M. Koiwa, K. Otsuka and T. Miyazaki, Japan Institute for Metals, Kyoto, Japan (1999) 1445-1452.
10. Jones, S. J. and Bhadeshia, H. K. D. H.: *Acta Materialia* **45** (1997) 2911-2920.
11. Jones, S. J. and Bhadeshia, H. K. D. H.: *Metallurgical and Materials Transactions A* **28A** (1997) 2005-2013.
12. Kasuya, T., Ichikawa, K., Fuji, M. and Bhadeshia, H. K. D. H.: *Materials Science and Technology* **15** (1999) 471-473.
13. Fujita, N. and Bhadeshia, H. K. D. H.: *Materials Science and Technology* **17** (2001) 403-408.
14. Fujita, N. and Bhadeshia, H. K. D. H.: *ISIJ International* **42** (2002) 760-767.
15. Fujita, N. and Bhadeshia, H. K. D. H.: *Advanced Heat Resistant Steels for Power Generation,* San Sebastian, published by the Institute of Materials, London (1998) 223-233.
16. Bhadeshia, H. K. D. H.: *Materials Science and Technology* **5,** (1989) 131-137.
17. Robson, J. R.: *Ph.D. Thesis,* University of Cambridge (1996)
18. Muruganath M. and Bhadeshia, H. K. D. H.: *Mathematical Modelling of Weld Phenomena 6,* eds H. Cerjak and H. K. D. H. Bhadeshia, Maney Publishers, London (2002) 243-260.
19. MacKay, D. J. C.: *Neural Computation* **4** (1992) 415-447.
20. MacKay, D. J. C.: *Neural Computation* **4** (1992) 448-472.
21. Bhadeshia, H. K. D. H. : *ISIJ International* **39** (1999) 966-979.
22. Lundin, C. D., Kelley, S. C., Menon, R. and Kruse, B. J.: *Welding Research Council bulletin 277,* New York (1986) 1-66.
23. Naoi, H., Mimura, H., Ohgami, M., Morimoto, H., Tanaka, T., Yazaki, Y. and Fujita, T.: *New Steels for Advanced Plant up to 620°C,* ed. E. Metcalfe, EPRI, California (1995) 8-29.
24. Downs, C., Hutchinson, J., Conroy, R. and Bhadeshia, H. K. D. H.: *Unpublished research* (2001)

❑